Metabolic preference of nitrate over oxygen as an electron acceptor in foraminifera from the Peruvian oxygen minimum zone

Nicolaas Glock[a,1], Alexandra-Sophie Roy[b], Dennis Romero[c], Tanita Wein[b], Julia Weissenbach[b,2], Niels Peter Revsbech[d], Signe Høgslund[e], David Clemens[a], Stefan Sommer[a], and Tal Dagan[b]

[a]Marine Geosystems, GEOMAR Helmholtz Centre for Ocean Research Kiel, 24148 Kiel, Germany; [b]Institute of Microbiology, Kiel University, 24118 Kiel, Germany; [c]Dirección General de Investigaciones Oceanográficas y Cambio Climático, Instituto del Mar del Perú, Callao 01, Peru 17; [d]Aarhus University Centre for Water Technology, Department of Bioscience, Aarhus University, DK-8000 Aarhus C, Denmark; and [e]Section of Marine Ecology, Department of Bioscience, Aarhus University, DK-8000 Aarhus C, Denmark

Benthic foraminifera populate a diverse range of marine habitats. Their ability to use alternative electron acceptors—nitrate (NO_3^-) or oxygen (O_2)—makes them important mediators of benthic nitrogen cycling. Nevertheless, the metabolic scaling of the two alternative respiration pathways and the environmental determinants of foraminiferal denitrification rates are yet unknown. We measured denitrification and O_2 respiration rates for 10 benthic foraminifer species sampled in the Peruvian oxygen minimum zone (OMZ). Denitrification and O_2 respiration rates significantly scale sublinearly with the cell volume. The scaling is lower for O_2 respiration than for denitrification, indicating that NO_3^- metabolism during denitrification is more efficient than O_2 metabolism during aerobic respiration in foraminifera from the Peruvian OMZ. The negative correlation of the O_2 respiration rate with the surface/volume ratio is steeper than for the denitrification rate. This is likely explained by the presence of an intracellular NO_3^- storage in denitrifying foraminifera. Furthermore, we observe an increasing mean cell volume of the Peruvian foraminifera, under higher NO_3^- availability. This suggests that the cell size of denitrifying foraminifera is not limited by O_2 but rather by NO_3^- availability. Based on our findings, we develop a mathematical formulation of foraminiferal cell volume as a predictor of respiration and denitrification rates, which can further constrain foraminiferal biogeochemical cycling in biogeochemical models. Our findings show that NO_3^- is the preferred electron acceptor in foraminifera from the OMZ, where the foraminiferal contribution to denitrification is governed by the ratio between NO_3^- and O_2.

eukaryotic denitrification | foraminifera | oxygen minimum zone | nitrogen cycle

Bioavailable nitrogen (N) is an essential building block of amino and nucleic acids in all living organisms (1). Nitrate (NO_3^-) is the most abundant form of reactive inorganic N within the oceans and a limiting nutrient for primary productivity within the surface ocean (2–4). The two main sinks for bioavailable N within the oceans are heterotrophic denitrification (i.e., the reduction of NO_3^- to N_2 during organic matter degradation) and anaerobic ammonium (NH_4^+) oxidation (anammox) (5–7). About 20–40% of the oceanic N loss takes place in oxygen minimum zones (OMZs), making them key regions for global oceanic nutrient cycling (2, 4, 8).

Benthic foraminifera are able to use NO_3^- as an electron acceptor for denitrification, which is a rare ability among eukaryotes (9–11). The only other eukaryotes known to date to perform incomplete denitrification of NO_3^- are two fungi (12) and the protist *Loxodes* (13). Additional eukaryotes that are able to use NO_3^- as an electron acceptor are two diatom species, which perform dissimilatory NO_3^- reduction to NH_4^+ (DNRA) (14, 15). Notably, benthic foraminifera are the only eukaryotes known to perform complete denitrification to N_2 gas (9, 15). While denitrification seems to be performed by

endobionts in some groomiid and allogromiid species (16, 17), some rotaliids surely have an eukaryotic denitrification pathway (18, 19). A recent study of the enzymes involved in the foraminiferal denitrification pathway in rotaliids showed that they are of an ancient prokaryotic origin (19). The uptake of NO_3^- and O_2 in foraminifera is likely facilitated by the pores present in the foraminiferal tests, whereas the pore density can be used as a quantitative NO_3^- proxy [e.g., in *Bolivina spissa* (20–22)]. Recent studies estimated that foraminifera account for a major part of benthic denitrification in OMZs due to their high abundance in those habitats and their contribution to biological NO_3^- transport (11, 23, 24). In the Peruvian OMZ, foraminifera and sulfur bacteria that perform DNRA compete for the available NO_3^- (23–25). The latter process produces NH_4^+ that feeds the environment with reactive N. The NH_4^+ can subsequently be removed by anammox either by benthic endosymbiotic bacteria or in the water column (26, 27). Anammox appears to be the main pelagic sink for dissolved reactive N in the Peruvian OMZ (28). These complex interactions pinpoint the importance of benthic foraminiferal denitrification for the global N cycling. Nevertheless, species-specific foraminiferal denitrification rates are very scarce in the literature and the measured rates vary by one to two orders of magnitude (9–11, 29, 30). Equally less is known about foraminiferal O_2 respiration rates (11, 31–38). Thus,

Significance

Foraminifera are able to respire nitrate instead of oxygen, a rare ability amongst eukaryotes. Here, we show that benthic foraminifera from the Peruvian oxygen minimum zone are not just facultative anaerobes by switching to nitrate respiration when oxygen is depleted but that denitrification is their preferred respiration pathway. Their metabolic adaptations allow some species to grow larger than predicted by cell physiology of aerobic organisms due to oxygen limitation. Finally, we formulate, from our observations, mathematical equations to predict the amount of foraminiferal denitrification using their cell volume. Nitrate is an important macronutrient, and denitrification is the main oceanic nitrate sink. Our equations will help to constrain biogeochemical models for marine nitrate cycling.

additional rate measurements are crucial to calculate sound estimates for the total benthic foraminiferal denitrification rates and to constrain the role of foraminifera in benthic O_2 respiration and carbon degradation.

Various characteristics of organisms, from energy consumption to population growth rate, are known to correlate with body size (39). The scaling of these characteristics with body size is well described by a power function with a scaling exponent α (39). The function is considered superlinear if α > 1, linear if α = 1 and sublinear if α < 1. According to "Kleiber's law," the scaling of metabolic rates with body size in mammals and birds is sublinear (α = 0.75) (40). Nonetheless, recent studies showed that the scaling of metabolic rates with body size varies among different taxa. Metabolic scaling is superlinear in prokaryotes, linear in protists, and sublinear in metazoans (39). At extremely large cell sizes, α decreases for prokaryotes and protists, leading to an overlap between large prokaryotes and small protists as well as between large protists and small metazoans. The larger classes of organisms are more efficient and competitive at larger body sizes, because more complex respiratory systems help to sustain higher demands for electron acceptors (39). Notably, the concept of metabolic scaling is useful to compare the efficiency between different metabolic pathways. Thus, when the rate of different metabolic pathways within a taxon—e.g., O_2 respiration and denitrification—scale with different exponents (α), the pathway with the larger α is considered to be more efficient.

Here, we determined rates of denitrification and O_2 respiration in benthic foraminifera from the Peruvian OMZ. We analyzed the relationship between these metabolic rates and the individual cell volume and the surface to volume ratio of the foraminifera. Finally, we tested for a metabolic preference between denitrification and O_2 respiration in foraminifera from OMZs by comparing the metabolic scaling of the two processes.

Results

Foraminiferal Denitrification Rates. Denitrification rates were measured for nine benthic foraminiferal species from the Peruvian OMZ ($n = 34$; *SI Appendix*, Tables S1 and S2). Active denitrification was determined in all 34 incubations, whereas all negative controls and blanks showed no N_2O production, i.e., no denitrification (*SI Appendix*, Fig. S1). Here, we term the metabolic rate of a single foraminifer "individual rate," while the term "specific rate" refers to the rate normalized by the cell volume. Our results show that the individual denitrification rates were significantly positively correlated with cell volume (Fig. 1A; $R^2 = 0.49$; $F = 30$; $P < 0.0001$; power regression). Additionally, the specific denitrification rates and the cell volume were weakly correlated (Fig. 1B; $R^2 = 0.18$; $F = 6.6$; $P = 0.015$). The correlation between cell volume and individual denitrification rates can be described according to Eq. **1**:

$$\ln\left(R_{den(ind)}\right) = 0.68 \cdot \ln(V_{bio}) - 5.57 \quad \text{or}$$
$$R_{den(ind)} = 3.80E-3 \cdot V_{bio}^{0.68}, \quad \text{[1]}$$

where $R_{den(ind)}$ is the individual denitrification rate in pmol individual (ind)$^{-1}$ d^{-1}, and V_{bio} is the cell volume in μm³. We note that throughout the presented statistical analyses, all underlying assumptions of the power regression are fulfilled unless mentioned otherwise (*SI Appendix*, Table S3). We further found a significant correlation between individual denitrification rates and the water depth where the foraminifera individuals were sampled; this observation may be explained by the higher abundance of larger foraminifera in deeper water depth (*SI Appendix*, Fig. S2A; $R^2 = 0.53$; $F = 37$; $P < 0.0001$; power regression).

Foraminiferal O_2 Respiration Rates. Oxygen respiration rates were determined for nine benthic foraminiferal species from the Peruvian OMZ and two additional species from the hypoxic Alsbäck deep of the Gullmar Fjord, Sweden ($n = 24$; *SI Appendix*, Table S4). The mean respiration rates measured within this study are within the range of the O_2 respiration rates previously published for other
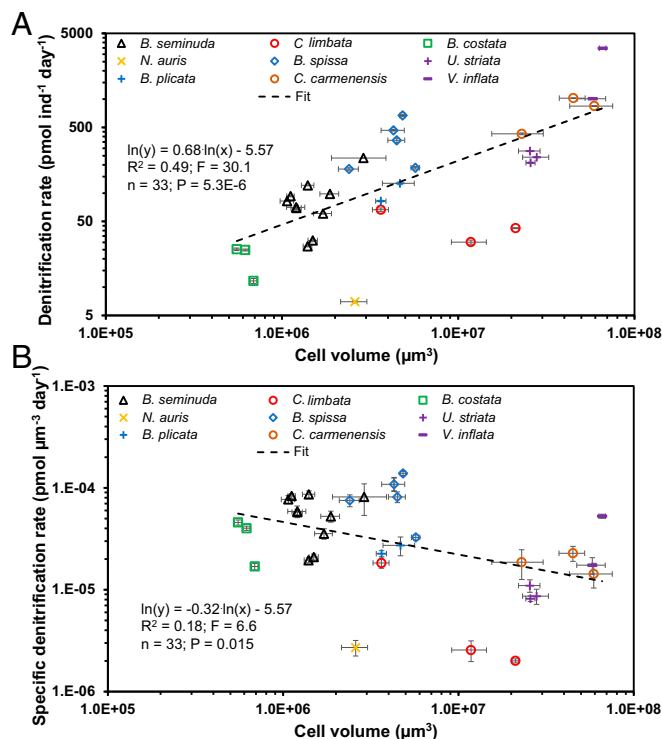

Fig. 1. Log–log plots and power regressions for individual foraminiferal denitrification rates (A) and volume-specific foraminiferal denitrification rates (B) against cell volume for benthic foraminifera from the Peruvian OMZ. Error bars are SEM (1SEM). "Individual rate" refers to the rate per single foraminifer. The cell volume is the mean individual cell volume in each incubation.

foraminiferal species (*SI Appendix*, Table S5). To test for a correlation between individual O_2 respiration rates and cell volume, we normalized all O_2 respiration rates from the literature according to the temperature present during the experiments (Fig. 2). Fitting a power regression to the whole dataset, including data from the literature and our measurements, revealed that the individual O_2 respiration rates were significantly positively correlated with the cell volume (Fig. 2A; $R^2 = 0.70$; $F = 183$; $P < 0.0001$; power regression). In contrast, the volume-specific O_2 respiration rates were significantly negatively correlated with cell volume (Fig. 2B; $R^2 = 0.46$; $F = 68$; $P < 0.0001$; power regression). The correlation between cell volume and individual O_2 respiration rates can be described according to Eq. **2**:

$$\ln\left(R_{Ox(ind)}\right) = 0.62 \cdot \ln(V_{bio}) - 3.50 \quad \text{or}$$
$$R_{Ox(ind)} = 3.03E-2 \cdot V_{bio}^{0.62}, \quad \text{[2]}$$

where $R_{Ox(ind)}$ is the individual O_2 respiration rate in pmol ind^{-1} d^{-1} (and V_{bio} as above). The correlation between cell volume and the volume-specific O_2 respiration rates [$R_{Ox(vol)}$] is described according to Eq. **3**:

$$\ln\left(R_{Ox(vol)}\right) = -0.38 \cdot \ln(V_{bio}) - 3.54 \quad \text{or}$$
$$R_{Ox(vol)} = 2.90E-2 \cdot V_{bio}^{-0.38}. \quad \text{[3]}$$

To further characterize the relation of O_2 respiration rates and cell volume in species from strongly O_2-depleted habitats, we divided the available O_2 respiration data into another subset. This dataset includes the data available for species from the Peruvian OMZ, including our data and data by Piña-Ochoa et al. (11). Our results show that the individual O_2 respiration rate in the Peruvian dataset is significantly positively correlated with cell volume, and yet the slope is much smaller in comparison with that within the dataset,
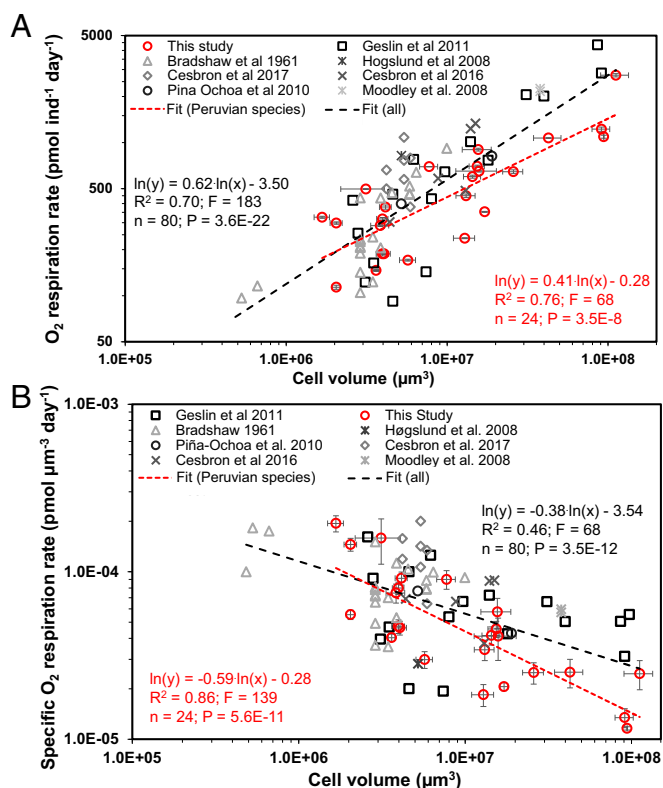
Fig. 2. Log–log plots for individual foraminiferal O_2 respiration rates (A) and volume-specific foraminiferal O_2 respiration rates (B) against cell volume for benthic foraminifera from the Peruvian OMZ and compared with the literature. The regressions are shown globally for all available data points (all) and for the Peruvian OMZ only. Error bars are 1 SEM. The data for each replicate are shown when available, but some data points consist only of averages for each species (10, 11, 36). The rates of ref. 33 were not included due to their exceptionally high values. "Individual rate" refers to the rate per single foraminifer. The cell volume is the mean individual cell volume in each incubation. The legends denoting the symbols in A and B cite the following references: Bradshaw et al. (31), Cesbron et al. (38), Piña-Ochoa et al. (29), Geslin et al. (36), Høgslund et al. (10), Cesbron et al. (37), and Moodley et al. (35).

which includes all of the species, even the ones from well-oxygenated environments (Fig. 2A). A comparison of the volume-specific O_2 respiration rates in both datasets showed that the negative slope with cell volume is steeper for the Peruvian species (Fig. 2B). Additionally, the individual O_2 respiration rates and water depth were significantly positively correlated for the Peruvian species (*SI Appendix*, Fig. S2B; $R^2 = 0.25$; $F = 6.8$; $P = 0.017$; power regression). This correlation may be linked to the higher abundance of larger foraminifera in deeper water depths.

The Ratio of Denitrification and O_2 Respiration. Combining the rates of denitrification and O_2 respiration measured for the Peruvian species showed that the ratio of species-specific denitrification and O_2 respiration rates increased with the water depth that is typical for the sampled species (Fig. 3). "Species-specific" refers to the mean value of an individual from a specific species. The species-specific denitrification/O_2 respiration ratio revealed a similar relation with water depth as the $[NO_3^-]/[O_2]$ ratios during the sampling period (Fig. 3).

Cell Volumes and Surface/Volume Ratios. The cell volume dependency to electron acceptor availability was evaluated by testing for a correlation between individual cell volume, water depth, and electron-acceptor concentration. This revealed that the individual cell volume of the foraminifera analyzed here is significantly

positively correlated with the water depth at the sampling location (*SI Appendix*, Fig. S3A; $R^2 = 0.47$; $F = 361$; $P < 0.0001$; logarithmic regression). The presence of *Bolivina seminuda* in samples from a wide range of water depths enabled us to further test for the above correlation within a single species. This revealed that the mean *B. seminuda* cell volume was significantly positively correlated with water depth at the sampling location (*SI Appendix*, Fig. S3B; $R^2 = 0.77$; $F = 55$; $P < 0.0001$; logarithmic regression). The observation adds further support to the observed positive correlation between foraminiferal cell size and water depth. Notably, the distribution of individual cell volumes for all analyzed species is comparable to the distribution of dissolved $[NO_3^-]$ at 12°S off Peru (*SI Appendix*, Fig. S4A). Furthermore, the correlation between the mean individual foraminiferal cell volume and the mean $[NO_3^-]$ measured in the same water depth was significantly positively correlated ($R^2 = 0.84$; $F = 32$; $P = 0.001$; *SI Appendix*, Fig. S4B; logarithmic regression). Similarly, the volume-specific O_2 respiration rate was significantly positively correlated with the surface/volume ratio of the individual foraminiferal tests (Fig. 4; $R^2 = 0.84$; $F = 104$; $P < 0.0001$; power regression). Additionally, we observed a weak but significant positive correlation between the volume-specific denitrification rates and the surface/volume ratio of the test (Fig. 4; $R^2 = 0.25$; $F = 10$; $P = 0.003$; power regression).

Discussion

Metabolic Preference for Denitrification over O_2 Respiration. Our results reveal a positive correlation of the individual rates of denitrification and O_2 respiration to the cell volume as described by the power law equations Eqs. **1** and **2** (Figs. 1A and 2A). These equations are a valuable tool to further constrain foraminiferal denitrification and O_2 respiration rates in biogeochemical models for marine NO_3^- and C cycling. Data for species-specific rates of benthic foraminifera are limited in the literature. Additionally, the scaling of such functions can be used to determine if foraminifera have a metabolic preference for denitrification or O_2 respiration. The exponent in the power law relationship between foraminiferal O_2 respiration and cell volume (Eq. **2**) is sublinear ($\alpha < 1$). Such sublinear metabolic scaling can be found for a wide range of organisms (40, 41). A recent study argued that the sublinear scaling ($\alpha < 1$) does not extend to protists (α, ~1) (39). However, foraminifera are relatively large protists, where the bigger species overlap in size with many metazoans. The metabolic rates observed in large protists and small metazoans are similar as well. Consequently, it has been hypothesized that the decrease in metabolic scaling in large protists is related to the increased demand of electron acceptors to the respiratory complexes. In large
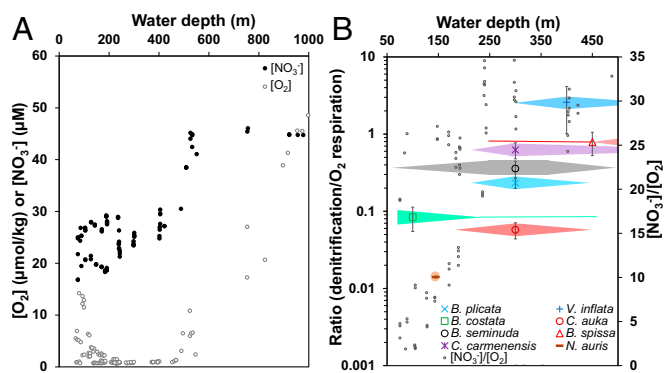

Fig. 3. (A) Distribution of near bottom water $[O_2]$ and $[NO_3^-]$ at 12°S within the Peruvian OMZ during cruise M137. (B) Ratios of $[NO_3^-]/[O_2]$ from A and ratios of mean species-specific denitrification/O_2 respiration rates for benthic foraminifera from the Peruvian OMZ in relationship to the living depth of the different species. "Species-specific" refers to the mean value of an individual from a species. The color fields represent the relative abundances of living specimens from these species within the different water depths. Abundances are taken from refs. 23 and 53.
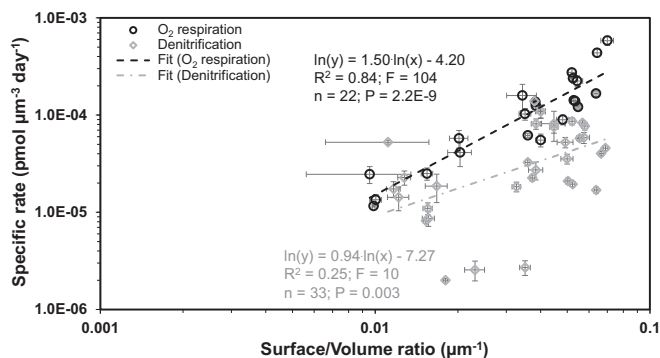
Fig. 4. Log–log plots and power regressions for volume-specific foraminiferal denitrification and O_2 respiration rates against surface/volume ratios for benthic foraminifera from the Peruvian OMZ. Error bars are 1 SEM.

protists, the cell volume and number of mitochondria are increased; however, their cell surface area is a limiting factor for the uptake of resources from the environment (39). The Peruvian OMZ is one of the most O_2-depleted regions in the world's oceans (42). Indeed, the O_2 respiration rates of foraminifera from the Peruvian OMZ scale with the cell volume with a much lower exponent ($\alpha = 0.41$; Fig. 2A) in comparison with the dataset from an earlier study, which mostly contains species from more oxygenated environments (from ref. 36 excluding our data from Peru: $\alpha = 0.80$). Consequently, we conclude that the Peruvian species metabolize O_2 less efficiently compared with species from other regions. We further show that the exponent for individual denitrification ($\alpha = 0.68$, Fig. 1A) is higher than the exponent calculated for O_2 respiration in the Peruvian species ($\alpha = 0.41$; Fig. 2A). This indicates that denitrification is more efficient than O_2 respiration in species from the Peruvian OMZ.

The foraminiferal volume-specific O_2 respiration rate significantly decreases with cell volume (Fig. 2B). This finding is in agreement with earlier reports in the literature (33). We suggest that this negative correlation is related to the decrease of the surface/volume ratio with increasing cell volume, which is a limiting factor for O_2 uptake. Indeed, the volume-specific O_2 respiration rates were positively correlated with the individual surface/volume ratio (Fig. 4). Notably, the volume-specific O_2 respiration rate of the Peruvian species decreased with cell volume with a steeper slope compared with the general trend found for foraminifera, including species from oxygenated habitats (Fig. 2B). This indicates that the Peruvian species are unable to sustain an increased O_2 supply with an increase in cell size. However, we note that the O_2 respiration rates we measured here are potential rates because most of the presented Peruvian species reside within a permanently anoxic habitat. Our results further revealed that the volume-specific O_2 respiration rates of the Peruvian species scales more strongly with their cell volume and their surface/volume ratio in comparison with their volume-specific denitrification rate (Figs. 1B, 2B, and 4). This might be explained by the supply pathway of the two electron acceptors to the respiratory complex. Since O_2 cannot be stored in the cell, its supply depends on the environmental $[O_2]$. In contrast, NO_3^- is readily available for denitrification through the intracellular NO_3^- storage. Consequently, the rate of denitrification is not expected to decrease in bigger cells due to a decrease in surface to volume ratio. We further hypothesize that the foraminifers even overcome the limitation of electron acceptor supply imposed by the outer cell surface area, by performing denitrification. The enigmatic observation that the cell volume of some foraminiferal species from the Santa Barbara Basin is negatively correlated with $[O_2]$ (43) can be explained by this availability of an alternative electron acceptor storage. Indeed, several foraminifera in that habitat have been shown to denitrify (18).

Foraminiferal Ecology and the Availability of Electron Acceptors. Our results indicate that the preference of denitrification over O_2 respiration strongly relies on the microhabitat of the foraminiferal species. The microhabitat is, among other parameters, characterized by different ratios of the electron acceptors NO_3^- and O_2 in the environment. Based on our findings, we propose a conceptual biogeochemical model describing foraminiferal denitrification in OMZs according to the environmental $[NO_3^-]/[O_2]$ ratio (Fig. 5; details in *SI Appendix, Note 1*). Foraminifera residing in the upper boundary of the Peruvian OMZ (Fig. 5A) showed a relatively low ratio of denitrification/O_2 respiration (Fig. 3B). The upper OMZ boundary is a highly fluctuating environment where the oxycline can vary between 0–125 m and strong O_2 intrusions from above are common at these water depths (44, 45). The bottom water $[NO_3^-]$ is relatively low (*SI Appendix, Figs. S4 and S5*) and can, during sulfidic events, be completely consumed (25) (*SI Appendix, Fig. S6*). Furthermore, mats of sulfur bacteria capable of performing DNRA are often clustered around the upper OMZ boundary (25, 46); hence, the competition for NO_3^- uptake in this region may be intense. The most common foraminiferal species living in these depths is the small *B. costata* (cell volume between 2×10^5 and $10 \times 10^5 \mu m^3$; $n = 67$). This species is characteristic for sulfidic sediments containing high amounts of labile organic matter, but it can also thrive in well-oxygenated sediments (45). From previous observations of *B. costata* (45), we can assert that species at the upper OMZ boundary are well adapted to fluctuations of the oxycline, periodic sulfidic conditions, and limited NO_3^- availability. In summary, foraminifera thriving in this environment are small, have a low ratio of denitrification/O_2 respiration, and, thus, generally have a low denitrification capacity, even if they occur in high abundances (Fig. 5A).

In contrast, foraminifera thriving at the lower OMZ boundary (Fig. 5C) have a relatively high denitrification/O_2 respiration ratio, indicating that they metabolize NO_3^- more efficiently than O_2. Indeed, the $[O_2]$ below the OMZ are variable, but only weakly, below 500 m water depth (47). The bottom water in these depths is considered to be anoxic most of the time (see also Fig. 3A and *SI Appendix, Figs. S5A and S6B*). Additionally, the $[NO_3^-]$ is relatively high at these depths due to the increase of $[NO_3^-]$ with water depth (*SI Appendix, Fig. S5C*). Competition for NO_3^- is restricted to the present foraminifers and to denitrifying bacteria. Some of the foraminiferal species present at these depths, e.g., *Cancris carmenensis* or *Valvulineria inflata*, can reach relatively large cell volumes (between 100×10^5 and $1,000 \times 10^5 \mu m^3$, $n = 24$). Notably, the intracellular NO_3^- uptake rate of foraminifera can be 10-fold higher than the denitrification rate (10). This observation further supports our notion according to which there is no limitation of electron acceptor uptake through the surface/volume ratio due to the availability of an intracellular NO_3^- storage. In summary, foraminifera can grow larger with increasing NO_3^- availability (thus water depth) and have an increasing denitrification capacity (Fig. 5 B and C).

The species-specific ratio of denitrification/O_2 respiration for the most abundant species at the Peruvian OMZ is directly coupled to the availability of NO_3^- and O_2 within their habitat (Fig. 3B). Our results indicate that the availability of different electron acceptors influences the community structure, and thus the ecology of benthic foraminifera. Even within individual species, the cell volume can be a plastic phenotypic trait that can depend on the electron acceptor concentration in the environment, as shown for *B. seminuda* (*SI Appendix, Fig. S3*). Benthic foraminifera are known to widely disperse as small juveniles or propagules and to form propagule banks in sediments (48). These banks contain abundant and diverse foraminiferal propagules that grow to maturity when exposed to the appropriate environmental conditions (48, 49). We hypothesize that the availability of different electron acceptors constitutes an additional selecting factor for the composition of species that develop from a propagule bank, in addition to other factors such as water depth, salinity, pH, and organic matter (C_{org}) supply. Indeed, the influence of O_2 and C_{org} on the distribution of foraminifera in benthic microhabitats has been described by the conceptual trophic oxygen model (50). A later study pointed out that the influence of alternative electron acceptors (NO_3^- in particular) (51) should be considered as well. Thus, species having high species-specific denitrification rates, like *C. carmenensis* and *V. inflata*, could develop
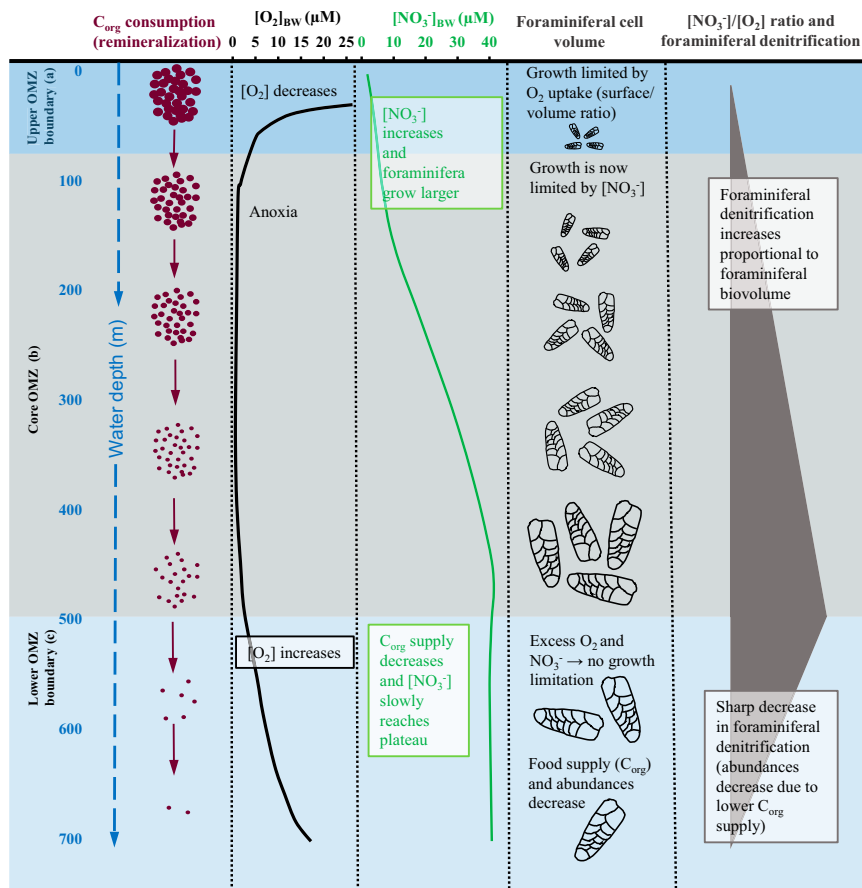
Fig. 5. Conceptual model for benthic foraminiferal denitrification at the Peruvian OMZ. A detailed description of the model is presented in *SI Appendix, Note 1*. (*A*) Upper OMZ boundary within the lower productive mixed layer: high C_{org} fluxes and O_2 consumption, low $[NO_3^-]$, high foraminiferal abundances, small foraminifera → Low $[NO_3^-]/[O_2]$ ratios and low total benthic foraminiferal denitrification. (*B*) Anoxic OMZ core: C_{org} fluxes decrease with water depth due to remineralization, while $[NO_3^-]$ increases, which results in larger foraminifera. Depletion of O_2 facilitates C_{org} preservation in the sediments, causing increased foraminiferal abundances. All this causes high $[NO_3^-]/[O_2]$ ratios and high total benthic foraminiferal denitrification, both increasing with water depth. (*C*) Lower OMZ boundary: C_{org} fluxes are decreasing because most C_{org} is already remineralized in the water column above. While $[O_2]$ gradually increases with water depth, $[NO_3^-]$ reaches a plateau. Foraminiferal abundances decrease due to decreased C_{org} within the sediments. This results in a sharp decrease of $[NO_3^-]/[O_2]$ ratios and total benthic foraminiferal denitrification with water depth. $[NO_3^-]$ and $[O_2]$ have been schematized after the data shown in the *SI Appendix*, Fig. S4.

when $[NO_3^-]$ is high and competition for NO_3^- uptake is low. Other species can grow to larger cell size due to increased $[NO_3^-]$ (*SI Appendix,* Fig. S3*B*). Such a community composition might lead to increased denitrification in the habitat. Furthermore, in habitats where NO_3^- is scarce and competition for NO_3^- uptake high (e.g., due to the presence of sulfur bacteria), species with a low species-specific denitrification rates (i.e., smaller species) would be favored. Consequently, the total foraminiferal denitrification is expected to decrease as NO_3^- availability will become a limiting factor for the total benthic denitrification. Our data, in combination with data of an earlier study (23) suggest that the ratio of foraminiferal denitrification over bacterial denitrification is around 20–50% within the Peruvian OMZ core but only 5% below the lower OMZ boundary (*SI Appendix, Note 2* and Table S8).

Conclusions

Benthic foraminifera are able to perform complete denitrification (9, 11). Nevertheless, benthic foraminifera from O_2-depleted environments have always been considered only as facultative anaerobes. Here, we compared the scaling of denitrification and O_2 respiration rates of benthic foraminifera from the Peruvian OMZ to their cell volume. Our findings reveal that benthic foraminifera from the Peruvian OMZ are not only able to survive under anoxia, rather, they find favorable conditions in such environments. In contrast to foraminifera from more oxygenated environments, the Peruvian species studied here show a metabolic preference for denitrification over O_2 respiration. Consequently, these species are better described as facultative aerobes rather than facultative anaerobes.

Methods

Sampling of Living Foraminifera. Sixteen short-sediment cores from the Peruvian OMZ were retrieved during Research Vessel (R/V) Meteor cruise M137

(May 2017) using a video-guided multiple corer (inner tube diameter, 10 cm). A map with the sampling locations is shown in the *SI Appendix,* Fig. S6 and Table S6. After retrieval, the supernatant water of each core was removed and the top 3 cm of sediment sliced in 1-cm intervals. The sediment core slices were immediately sieved through a 63-μm mesh using fresh surface seawater, and the 63- to 2,000-μm fraction was collected in polypropylene beakers. Living foraminiferal specimens within this residue were identified according pseudopodial activity as well as cytoplasm abundance and color based on a live/dead CellTracker Green fluorescent dye (ThermoFisher) assessment of each species. Viable foraminiferal specimens were cleaned with a brush and washed twice in NO_3^--free artificial seawater (Red Sea Salt), directly before rate measurements incubations. Typically, it took 60–90 min after core retrieval before specimens were incubated for rate measurements.

Determination of Foraminiferal Denitrification and O_2 Respiration Rates. Foraminiferal denitrification and O_2 respiration rates were calculated from linear steady-state gradients of nitrous oxide (N_2O) or O_2 in glass microcapsules (9–11, 29). For each experiment, 4–13 specimens were incubated. The number of specimens depended on the size of the randomly selected living individuals. In total, 34 incubations for the determination of denitrification rates and 24 incubations for the determination of O_2 respiration rates were made, excluding the negative control and blanks. Negative controls were done by measuring rates from chambers with empty foraminiferal tests and blanks with empty chambers. Both negative control and blank showed no N_2O production after acetylene inhibition (52) (*SI Appendix,* Fig. S1). For more details about the determination of the denitrification and O_2 respiration rates, see *SI Appendix, Note 3*.

Cell Volume Determination. We estimated the total foraminiferal volume for each specimen according to ref. 36. The test volume was estimated by using the best resembling geometric shape (*SI Appendix,* Table S7) and the cell volume by the assumption that the internal test volume corresponds to 75% of the whole test volume and is completely filled with cytoplasm (33). For more details about the cell volume determination, see *SI Appendix, Note 4*.

Respiration Rates from Literature. All O_2 respiration rates from the literature were converted into pmol ind^{-1} d^{-1} and normalized to 13 °C according to the method described in ref. 36 to produce a sufficient database for data comparison. A more detailed description on how the literature data were treated is presented in *SI Appendix, Note 5*.

Environmental Data. [NO_3^-] and [O_2] in the benthic boundary layer were determined during 49 conductivity, temperature, and depth casts during cruise M137 within the same transect as the sediment samples were taken for the foraminiferal analyses. For more details, see *SI Appendix, Note 6*.

Statistics. Linear regressions were used to analyze our data after logarithmic and double logarithmic transformations. For statistical details, see *SI Appendix, Note 7 and Table S3*.

1. Gruber N, Galloway JN (2008) An Earth-system perspective of the global nitrogen cycle. *Nature* 451:293–296.
2. Gruber N (2004) The dynamics of the marine nitrogen cycle and its influence on atmospheric CO2 variations. *The Ocean Carbon Cycle and Climate* (Springer, Dordrecht, The Netherlands), pp 97–148.
3. Arrigo KR (2005) Marine microorganisms and global nutrient cycles. *Nature* 437:349–355.
4. Lam P, et al. (2009) Revising the nitrogen cycle in the Peruvian oxygen minimum zone. *Proc Natl Acad Sci USA* 106:4752–4757.
5. van de Graaf AA, et al. (1995) Anaerobic oxidation of ammonium is a biologically mediated process. *Appl Environ Microbiol* 61:1246–1251.
6. Thamdrup B, Dalsgaard T (2002) Production of N(2) through anaerobic ammonium oxidation coupled to nitrate reduction in marine sediments. *Appl Environ Microbiol* 68:1312–1318.
7. Kuypers MMM, et al. (2003) Anaerobic ammonium oxidation by anammox bacteria in the Black Sea. *Nature* 422:608–611.
8. Bohlen L, Dale AW, Wallmann K (2012) Simple transfer functions for calculating benthic fixed nitrogen losses and C:N:P regeneration ratios in global biogeochemical models. *Global Biogeochem Cycles* 26:GB3029.
9. Risgaard-Petersen N, et al. (2006) Evidence for complete denitrification in a benthic foraminifer. *Nature* 443:93–96.
10. Høgslund S, Revsbech NP, Cedhagen T, Nielsen LP, Gallardo VA (2008) Denitrification, nitrate turnover, and aerobic respiration by benthic foraminiferans in the oxygen minimum zone off Chile. *J Exp Mar Biol Ecol* 359:85–91.
11. Piña-Ochoa E, et al. (2010) Widespread occurrence of nitrate storage and denitrification among Foraminifera and Gromiida. *Proc Natl Acad Sci USA* 107:1148–1153.
12. Usuda K, Toritsuka N, Matsuo Y, Kim DH, Shoun H (1995) Denitrification by the fungus Cylindrocarpon tonkinense: Anaerobic cell growth and two isozyme forms of cytochrome P-450nor. *Appl Environ Microbiol* 61:883–889.
13. Finlay BJ, Span ASW, Harman JMP (1983) Nitrate respiration in primitive eukaryotes. *Nature* 303:333–336.
14. Kamp A, de Beer D, Nitsch JL, Lavik G, Stief P (2011) Diatoms respire nitrate to survive dark and anoxic conditions. *Proc Natl Acad Sci USA* 108:5649–5654.
15. Kamp A, Høgslund S, Risgaard-Petersen N, Stief P (2015) Nitrate storage and dissimilatory nitrate reduction by eukaryotic microbes. *Front Microbiol* 6:1492.
16. Bernhard JM, Edgcomb VP, Casciotti KL, McIlvin MR, Beaudoin DJ (2012) Denitrification likely catalyzed by endobionts in an allogromiid foraminifer. *ISME J* 6:951–960.
17. Høgslund S, Cedhagen T, Bowser SS, Risgaard-Petersen N (2017) Sinks and sources of intracellular nitrate in gromiids. *Front Microbiol* 8:617.
18. Bernhard JM, et al. (2012) Potential importance of physiologically diverse benthic foraminifera in sedimentary nitrate storage and respiration. *J Geophys Res Biogeosci* 117:G03002.
19. Woehle C, et al. (2018) A novel eukaryotic denitrification pathway in foraminifera. *Curr Biol* 28:2536–2543.e5.
20. Glock N, et al. (2011) Environmental influences on the pore-density in tests of Bolivina spissa. *J Foraminiferal Res* 41:22–32.
21. Glock N, Schönfeld J, Mallon J (2012) The functionality of pores in benthic foraminifera in view of bottom water oxygenation: A review. *Anoxia: Evidence for Eukaryote Survival and Paleontological Strategies*, eds Altenbach AV, Bernhard JM, Seckbach J (Springer, Dordrecht, The Netherlands), (2012) 537–552.
22. Glock N, et al. (2018) Coupling of oceanic carbon and nitrogen facilitates spatially resolved quantitative reconstruction of nitrate inventories. *Nat Commun* 9:1217.
23. Glock N, et al. (2013) The role of benthic foraminifera in the benthic nitrogen cycle of the Peruvian oxygen minimum zone. *Biogeosciences* 10:4767–4783.
24. Dale AW, Sommer S, Lomnitz U, Bourbonnais A, Wallmann K (2016) Biological nitrate transport in sediments on the Peruvian margin mitigates benthic sulfide emissions and drives pelagic N loss during stagnation events. *Deep Sea Res Part I* 112:123–136.
25. Sommer S, et al. (2016) Depletion of oxygen, nitrate and nitrite in the Peruvian oxygen minimum zone cause an imbalance of benthic nitrogen fluxes. *Deep Sea Res Part I* 112:113–122.
26. Prokopenko MG, et al. (2013) Nitrogen losses in anoxic marine sediments driven by Thioploca-anammox bacterial consortia. *Nature* 500:194–198.
27. Dale AW, Bourbonnais A, Altabet M, Wallmann K, Sommer S (2019) Isotopic fingerprints of benthic nitrogen cycling in the Peruvian oxygen minimum zone. *Geochim Cosmochim Acta* 245:406–425.
28. Kalvelage T, et al. (2013) Nitrogen cycling driven by organic matter export in the South Pacific oxygen minimum zone. *Nat Geosci* 6:228–234.
29. Piña-Ochoa E, Koho KA, Geslin E, Risgaard-Petersen N (2010) Survival and life strategy of the foraminiferan Globobulimina turgida through nitrate storage and denitrification. *Mar Ecol Prog Ser* 417:39–49.
30. Bernhard JM, et al. (2012) Potential importance of physiologically diverse benthic foraminifera in sedimentary nitrate storage and respiration. *J Geophys Res Biogeosci* 117:G03002.
31. Bradshaw JS (1961) Laboratory experiments on the ecology of foraminifera. *Contrib Cushman Found Foraminiferal Res* 12:87–106.
32. Lee JJ, Muller A (1973) Trophic dynamics and niches of salt marsh foraminifera. *Am Zool* 13:215–223.
33. Hannah F, Rogerson A, Laybourn-parry J (1994) Respiration rates and biovolumes of common benthic foraminifera (Protozoa). *J Mar Biol Assoc UK* 74:301–312.
34. Nomaki H, Yamaoka A, Shirayama Y, Kitazato H (2007) Deep-sea benthic foraminiferal respiration rates measured under laboratory conditions. *J Foraminiferal Res* 37:281–286.
35. Moodley L, et al. (2008) Biomass-specific respiration rates of benthic meiofauna: Demonstrating a novel oxygen micro-respiration system. *J Exp Mar Biol Ecol* 357:41–47.
36. Geslin E, et al. (2011) Oxygen respiration rates of benthic foraminifera as measured with oxygen microsensors. *J Exp Mar Biol Ecol* 396:108–114.
37. Cesbron F, et al. (2016) Vertical distribution and respiration rates of benthic foraminifera: Contribution to aerobic remineralization in intertidal mudflats covered by Zostera noltei meadows. *Estuar Coast Shelf Sci* 179:23–38.
38. Cesbron F, et al. (2017) Sequestered chloroplasts in the benthic foraminifer Haynesina germanica: Cellular organization, oxygen fluxes and potential ecological implications. *J Foraminiferal Res* 47:268–278.
39. DeLong JP, Okie JG, Moses ME, Sibly RM, Brown JH (2010) Shifts in metabolic scaling, production, and efficiency across major evolutionary transitions in life. *Proc Natl Acad Sci USA* 107:12941–12945.
40. Kleiber M (1932) Body size and metabolism. *Hilgardia* 6:315–353.
41. Warwick RM, Price R (1979) Ecological and metabolic studies on free-living nematodes from an estuarine mud-flat. *Estuarine Coastal Mar Sci* 9:257–271.
42. Stramma L, Johnson GC, Sprintall J, Mohrholz V (2008) Expanding oxygen-minimum zones in the tropical oceans. *Science* 320:655–658.
43. Keating-Bitonti CR, Payne JL (2017) Ecophenotypic responses of benthic foraminifera to oxygen availability along an oxygen gradient in the California Borderland. *Mar Ecol* 38:e12430.
44. Gutiérrez D, et al. (2008) Oxygenation episodes on the continental shelf of central Peru: Remote forcing and benthic ecosystem response. *Prog Oceanogr* 79:177–189.
45. Cardich J, et al. (2015) Calcareous benthic foraminifera from the upper central Peruvian margin: Control of the assemblage by pore water redox and sedimentary organic matter. *Mar Ecol Prog Ser* 535:63–87.
46. Mosch T, et al. (2012) Factors influencing the distribution of epibenthic megafauna across the Peruvian oxygen minimum zone. *Deep Sea Res Part I* 68:123–135.
47. Sommer S, et al. (2010) Life at the edge–Oscillating lower boundary of the Peruvian oxygen minimum zone. Ocean Sciences Meeting 2010, February 22–26, 2010, Portland, OR. *EOS Transactions: Ocean Sciences Meeting Supplement*; abstr BO24C-08.
48. Alve E, Goldstein ST (2003) Propagule transport as a key method of dispersal in benthic foraminifera (Protista). *Limnol Oceanogr* 48:2163–2170.
49. Goldstein S, Alve E (2011) Experimental assembly of foraminiferal communities from coastal propagule banks. *Mar Ecol Prog Ser* 437:1–11.
50. Jorissen FJ, de Stigter HC, Widmark JGV (1995) A conceptual model explaining benthic foraminiferal microhabitats. *Mar Micropaleontol* 26:3–15.
51. Koho KA, Piña-Ochoa E (2012) Benthic foraminifera: Inhabitants of low-oxygen environments. *Anoxia: Evidence for Eukaryote Survival and Paleontological Strategies*, eds Altenbach AV, Bernhard JM, Seckbach J (Springer, Dordrecht, The Netherlands), pp 249–285.
52. Smith MS, Firestone MK, Tiedje JM (1978) The acetylene inhibition method for short-term measurement of soil denitrification and its evaluation using nitrogen-131. *Soil Sci Soc Am J* 42:611.
53. Mallon J (2012) Benthic foraminifera of the Peruvian & Ecuadorian continental margin. PhD thesis (Christian-Albrechts Universität zu Kiel, Kiel, Germany).

EARTH, ATMOSPHERIC, AND PLANETARY SCIENCES

PHYSIOLOGY